

High-purity Entanglement of Hot Propagating Modes using Nonreciprocity

L. Orr,¹ S. A. Khan,² N. Buchholz,¹ S. Kotler,³ and A. Metelmann^{1, 4, 5}

¹*Dahlem Center for Complex Quantum Systems and Fachbereich Physik,
Freie Universität Berlin, 14195 Berlin, Germany*

²*Department of Electrical Engineering, Princeton University, Princeton, NJ 08544, USA*

³*Racah Institute of Physics, The Hebrew University of Jerusalem, Jerusalem, 91904, Israel*

⁴*Institute for Theory of Condensed Matter, Karlsruhe Institute of Technology, 76131 Karlsruhe, Germany*

⁵*Institute for Quantum Materials and Technology,
Karlsruhe Institute of Technology, 76344 Eggenstein-Leopoldshafen, Germany*

(Dated: September 16, 2022)

Distributed quantum information processing and communication protocols demand the ability to generate entanglement among propagating modes of high purity. However, thermal fluctuations can severely limit the fidelity and purity of propagating entangled states, especially for low frequency modes relevant for radio-frequency (RF) signals. Here we propose nonreciprocity as a resource to render continuous-variables entanglement of propagating modes robust against thermal fluctuations. By utilizing a cold engineered reservoir we break the symmetry of reciprocity in a standard two-mode squeezing interaction between a low and a high frequency mode, and show that the re-routing of the thermal fluctuations allows the generation of flying entangled states with high purity. Our approach requires only pairwise Gaussian interactions and is thus ideal for parametric circuit QED implementations.

PACS numbers: 84.30.Le 03.65.Ta, 42.50.Pq 42.50.Lc

I. INTRODUCTION

Entanglement of propagating photons [1] is a crucial resource for quantum information processing and communication protocols [2] and is useful for distributing entanglement amongst components of a quantum network [3, 4]. However, as with other quantum-coherent effects, it is remarkably sensitive to decoherence channels, such as thermal fluctuations. Operating at cryogenic temperatures allows for the effects of thermal fluctuations to be overcome by ensuring that $k_b T \ll \hbar\omega$, which is possible for mode frequencies ω as low as the microwave domain [5]. For even lower frequency bands, such as the radio-frequency (RF) domain that is ubiquitous in modern communication, thermal fluctuations remain appreciable even at the coldest operating temperatures [6–8], presenting challenges for RF quantum communication and sensing. With these cryogenic temperature limitations, alternative approaches to generate entanglement in systems of hot modes must be considered.

In this paper, we present an approach utilizing engineered nonreciprocity to generate steady-state entangled output fields from a system of interacting hot modes coupled to a single cold mode. While several proposals and recent experiments consider the output field entanglement of cold modes via an intermediate hot (for example, mechanical) mode [9–14], we consider situations where the fields to be entangled themselves are effectively coupled to high temperature baths. Continuous ambient thermal excitations can severely limit the entanglement fidelity of steady-state emission from such ‘hot’ modes at a given pump power. Furthermore, these excitations limit the purity of the generated flying states, demanding

the use of complex state purification protocols [15–17]. We show that nonreciprocity provides a crucial ingredient to alleviate these effects: the ability to continuously reroute thermal excitations towards a cold output. This enables the entanglement of propagating photons with increased robustness to thermal excitations, and with much higher purity than possible using a completely reciprocal two-mode entangling interaction between the hot modes of interest.

The importance of nonreciprocity has already been firmly established in quantum information processing, enabling the routing of signals in a quantum network by realizing asymmetric scattering matrices, across diverse architectures from superconducting circuits [18–26] to optomechanics [27–31] and beyond [32, 33]. Our work analyzes a much less-explored aspect of nonreciprocal interactions: the role of nonreciprocity in manipulating *fluctuations* in a quantum system, to route thermal noise while generating entanglement of the scattered fields. Building on recent progress in the theory of engineered nonreciprocity [18, 34–36], we consider a system of three dissipative quantum modes undergoing configurable coherent interactions, and identify the conditions required for nonreciprocal scattering and directional transmission. Interestingly, by analyzing the complete output state we find that entanglement can be enhanced at points of ‘perfect nonreciprocity’, where scattering in one direction is forbidden. Perhaps equally as importantly, it is also possible to engineer nonreciprocal scattering between a pair of modes without entangling their outputs, highlighting the need for a deeper understanding of the connections between nonreciprocity and entanglement. To this end, we develop a heuristic picture drawing connections between steady-state entanglement in nonreciprocal systems and

sequential Gaussian circuit operations, as well as dissipative entanglement schemes [11, 37], and ideal two-mode squeezing.

Finally, we use this intuition to explain how nonreciprocal scattering impacts thermal fluctuations. We find that nonreciprocal scattering can be engineered to continuously re-route incident thermal excitations towards the output of the auxiliary cold mode introduced to break reciprocity. This results in an increase in entanglement fidelity and state purity of output fields scattered off the hot modes when compared to a reciprocal two-mode squeezing interaction between the modes at the same interaction strength. Our proposed three-mode system requires only pairwise squeezing and beam-splitter interactions, and can thus be efficiently realized in parametric circuit QED (cQED) [19, 21].

The rest of this paper is organized as follows. In Sec. II, starting with a two-mode squeezing interaction, we introduce the minimal three-mode system required to render this interaction nonreciprocal, within the context of standard approaches to nonreciprocity. In Secs. III and IV, we proceed to analyze the scattering and entangling properties of the three-mode system, finding conditions for nonreciprocal scattering, and clarifying the connection between nonreciprocity and entanglement generation. We find that at the specific points of ‘perfect nonreciprocity,’ the system’s scattering and entangling properties can be very efficiently explained as a sequence of simple pairwise linear operations. Finally, Sec. V combines this understanding to explore the impact of thermal fluctuations on entanglement in nonreciprocal systems, and demonstrates how thermal inputs to a hot mode can be efficiently routed via nonreciprocity to protect the entanglement of scattered output fields.

II. SETUP

We begin with the standard description of a nondegenerate squeezing interaction between two harmonic modes (setting $\hbar = 1$),

$$\hat{H}_{\text{TMS}} = g_{12} \left(\hat{a}_1^\dagger \hat{a}_2^\dagger + \hat{a}_1 \hat{a}_2 \right), \quad (1)$$

where \hat{a}_j is the bosonic annihilation operator for mode j , satisfying the standard commutation relations $[\hat{a}_j, \hat{a}_k^\dagger] = \delta_{jk}$. In a cQED architecture such an interaction is typically realized by appropriately pumping nonlinear Josephson-junction based superconducting elements [38, 39]. Additionally, this interaction can be used to generate entangled photon pairs [40] and hence two-mode squeezed light for quantum information processing applications [41, 42]. Nevertheless, the interaction defined by Eq. (1) is reciprocal.

The conditions required to render interactions of the form of Eq. (1) nonreciprocal have been clarified in recent years [35, 36]. An arbitrary bi-directional interaction between two systems, $\hat{H}_{\text{int}} \propto (\hat{A}\hat{B} + h.c.)$ governed by oper-

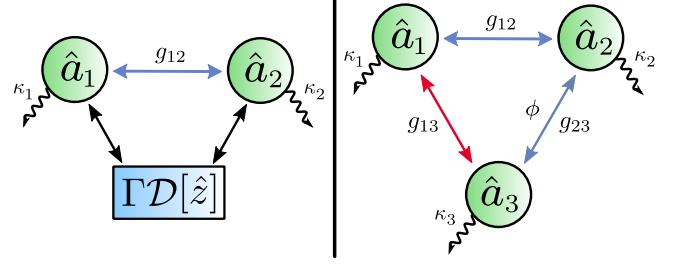


FIG. 1. [Left] Diagram of an open two-mode squeezer where both modes are coupled to the common non-local dissipator $\Gamma\mathcal{D}[\hat{z}]$. [Right] Diagram of a minimal loop system consisting of three open modes. Modes \hat{a}_1 and \hat{a}_2 are coupled via a two-mode squeezing interaction, as are modes \hat{a}_2 and \hat{a}_3 . Modes \hat{a}_1 and \hat{a}_3 are coupled via a beam-splitter interaction. The tunable loop phase is placed on the interaction between modes \hat{a}_2 and \hat{a}_3 . If mode \hat{a}_3 is adiabatically eliminated this loop is equivalent to the left diagram with the jump operator given by $\hat{z} = \hat{a}_1 + \eta e^{i\phi} \hat{a}_2^\dagger$.

ators \hat{A}, \hat{B} , must be balanced with a corresponding non-local dissipative interaction $\Gamma\mathcal{D}[\hat{z}]$ as depicted in Fig. 1, where $\mathcal{D}[\hat{z}]\hat{\rho} = \hat{z}\hat{\rho}\hat{z}^\dagger - \frac{1}{2}\{\hat{z}^\dagger\hat{z}, \hat{\rho}\}$ is the standard dissipative superoperator, with collapse operator $\hat{z} = \hat{A} + \eta e^{i\phi} \hat{B}$. An appropriately chosen interaction strength Γ , asymmetry η , and, most crucially, phase ϕ [36], can then be used to render the desired interaction nonreciprocal.

Applying this approach to the interaction defined by Eq. (1), it is clear that dissipators with either the collapse operator $\hat{z} = \hat{a}_1 + \eta e^{i\phi} \hat{a}_2^\dagger$ or $\hat{z} = \hat{a}_1^\dagger + \eta e^{-i\phi} \hat{a}_2$ both satisfy the aforementioned form, and can thus be employed to attain the desired nonreciprocal scattering matrix. Importantly, it has been shown that either dissipative interaction alone can generate steady-state entanglement [11, 37]. Hence, by combining either dissipator with the coherent two-mode squeezing interaction in Eq. (1), one can also take the point of view that we are analyzing the effects of introducing nonreciprocity in such dissipative entanglement schemes.

A hint as to what may be expected can be found in the fact that the required operators \hat{z} are *non-Hermitian* non-local collapse operators. Nonreciprocal interactions mediated by dissipators with Hermitian collapse operators have been shown to be equivalent to measurement-based feedforward schemes [36]: a classical observer makes a measurement on system A, and uses the result to evolve system B, breaking the reciprocity of interaction between the systems. As such, this evolution is equivalent to performing local operations and classical communication, and hence cannot generate any entanglement between the two quantum systems. In contrast, the non-Hermitian collapse operators required here have no such mapping, and can in principle generate entanglement.

To realize either non-local dissipator and hence render the TMS interaction nonreciprocal, we must introduce an auxiliary mode a_3 , as depicted in the right hand panel of Fig. 1. The open quantum system comprising this loop

and the environment it interacts with is described by the quantum-optical master equation:

$$\dot{\hat{\rho}} = \mathcal{L}\hat{\rho} = -i[\hat{H}_{\text{NRL}}, \hat{\rho}] + \sum_{j=1,2,3} \kappa_j \mathcal{D}[\hat{a}_j] \hat{\rho} \quad (2)$$

and its dynamics are governed by the Hamiltonian

$$\hat{H}_{\text{NRL}} = \left(g_{12}\hat{a}_1^\dagger \hat{a}_2^\dagger + g_{13}\hat{a}_3^\dagger [\hat{a}_1 + \eta e^{i\phi} \hat{a}_2^\dagger] \right) + \text{h.c.} \quad (3)$$

where $\eta = g_{23}/g_{13}$ accounts for an asymmetric coupling to the auxiliary mode, written in the interaction frame with respect to the three modes. Eq. (3) simply describes the original two-mode squeezing interaction between modes a_1 and a_2 , but now with an auxiliary third mode that couples to mode a_1 via a beam-splitter interaction, and to mode a_2 via a two-mode squeezing interaction. When the auxiliary mode a_3 can be adiabatically eliminated (namely, when its damping rate κ_3 is the largest system parameter), this configuration realizes the non-local dissipator $\hat{z} = \hat{a}_1 + \eta e^{i\phi} \hat{a}_2^\dagger$. Engineering the alternative non-local dissipator introduced earlier leads to equivalent results. The resulting three-mode system can thus render the interaction of Eq. (1) unidirectional and realize a nonreciprocal loop (NRL) via the general scheme described above.

By including the dynamics of the auxiliary mode we will be able to explore the routing of both scattered fields and - importantly - their correlations around the loop. In the remainder of this paper we will analyze how the engineered nonreciprocity of the system defined in Eq. (2) affects the quantum properties of the multimode output state, in particular its bipartite entanglement.

III. NONRECIPROCITY AND ENTANGLEMENT

When analysing the three-mode loop, we will restrict the initial state $\hat{\rho}_{\text{in}}$ of the system to Gaussian states. Each mode is equipped with a pair of quadrature operators, $\hat{X}_k = (\hat{a}_k^\dagger + \hat{a}_k)/\sqrt{2}$ and $\hat{P}_k = i(\hat{a}_k^\dagger - \hat{a}_k)/\sqrt{2}$ where $k \in \{1, 2, 3\}$. We can also define quadrature modes for the input or output states by replacing k with $(k, \text{in/out})$, respectively. By declaring the initial state $\hat{\rho}_{\text{in}}$ to be Gaussian, we mean that it is completely characterized by the first and second moments of these quadrature operators. Since the dynamics induced by the Hamiltonian in Eq. (3) is entirely linear, the state of the system at any time will also be Gaussian, including the output state $\hat{\rho}_{\text{out}}$ [43].

Our approach to analyzing the steady-state scattering properties of the system is standard: we solve the linear Heisenberg-Langevin equations in frequency space, and use quantum input-output theory [44], (see Appendix A). From this we obtain the scattering matrix $\mathbf{S}[\omega]$ relating output field operators to the input fields,

$$\vec{R}_{\text{out}}[\omega] = \mathbf{S}[\omega] \vec{R}_{\text{in}}[\omega]. \quad (4)$$

where $\vec{R}_{\text{in/out}}[\omega]$ is a vector of quadrature operators for the input and output modes, respectively.

We are interested in the scattering behaviour on resonance, that is when ($\omega = 0$) in this frame, which describes the response of fields resonant with the individual modes comprising the system. The scattering matrix in this simpler case, $\mathbf{S}[0] \equiv \mathbf{S}$, can be expressed purely in terms of the cooperativities $\mathcal{C}_{jk} = 4g_{jk}^2/\kappa_j \kappa_k$ parameterizing interactions between mode pairs (j, k) in relation to their individual decay rates. By balancing the cooperativities and adjusting the loop phase ϕ , scattering between any pair of modes in the system can be rendered nonreciprocal. The full form of the scattering matrix is still unwieldy (see Appendix B). We therefore introduce measures that allow us to quantify the system's scattering properties more compactly.

For nonreciprocal systems, we are primarily interested in the asymmetry of scattering between modes i and j . To more precisely quantify this asymmetry, we introduce the normalized degree of nonreciprocity $\mathcal{N}^{(i,j)}$ as

$$\mathcal{N}^{(i,j)} = \frac{\|\text{abs } \mathbf{S}^{(i,j)} - \text{abs } \mathbf{S}^{(j,i)}\|}{\|\mathbf{S}^{(i,j)}\| + \|\mathbf{S}^{(j,i)}\|} \quad (5)$$

where $\text{abs } \mathbf{O}$ is an element-wise absolute value operation, and $\|\cdot\|$ is the Frobenius norm. $\mathcal{N}^{(i,j)}$ is a quantity that remains bounded within $[0, 1]$, and measures the difference in *amplitude* (and not phase) of scattering between a pair of modes. As a result, it vanishes for scattering that is reciprocal in amplitude but which may differ in phase. As discussed in Appendix B, it can be shown that $\mathcal{N}^{(i,j)} = 0, \forall i \neq j$ only when $\phi = 0$.

For all other values of ϕ , the three-mode system exhibits nonreciprocal scattering properties to varying degrees. To understand how this nonreciprocity influences the quantum properties of scattered input fields, we can analyze the covariance matrix of the output fields. However, before analyzing the general case, we find that several key ideas can be understood via a simple heuristic picture that is valid where $\mathcal{N}^{(i,j)} = 1$. From Eq. (5), this corresponds to perfectly asymmetric scattering, where either $\|\mathbf{S}^{(i,j)}\|$ or $\|\mathbf{S}^{(j,i)}\|$ vanishes. We refer to these as points of *perfect* nonreciprocity, and the required conditions are summarized below. The arrows denote the direction in which signal transmission is allowed; scattering matrix elements in the reverse direction vanish exactly:

	$\phi = -\pi/2$	$\phi = +\pi/2$
$\mathcal{C}_{12} = \mathcal{C}_{13}\mathcal{C}_{23}$	$a_1 \rightarrow a_2$	$a_1 \leftarrow a_2$
$\mathcal{C}_{23} = \mathcal{C}_{12}\mathcal{C}_{13}$	$a_2 \rightarrow a_3$	$a_2 \leftarrow a_3$
$\mathcal{C}_{13} = \mathcal{C}_{12}\mathcal{C}_{23}$	$a_1 \rightarrow a_3$	$a_1 \leftarrow a_3$

(6)

In this work, we will pay particular attention to scattering between modes a_1 and a_2 , and hence set $\mathcal{C}_{12} = \mathcal{C}_{13}\mathcal{C}_{23}$. Plotting $\mathcal{N}^{(1,2)}$ in Fig. 2, we see that scattering between modes a_1 and a_2 can be rendered perfectly nonreciprocal, $\mathcal{N}^{(1,2)} = 1$, when $\phi = \pm\pi/2$.

A. Circuit decomposition at points of perfect nonreciprocal scattering

The scattering matrix describes a potentially complicated set of linear operations on Gaussian states. In order to more easily understand the scattering behaviour of the system, a variety decomposition schemes can be used to represent this set of operations more efficiently. One such prominent example is the Bloch-Messiah decomposition [45], a special case of the singular value decomposition for the group of real symplectic matrices of which the steady-state scattering matrix \mathbf{S} is an element, $\mathbf{S} \in Sp(2n, \mathbb{R})$.

We find that for the perfectly nonreciprocal system under consideration, the less-common *polar* decomposition proves to be simpler [46]. This decomposition allows us to write a symplectic matrix in the form $\mathbf{R}\mathbf{U}$, referred to as its left polar decomposition, where $\mathbf{U} \in Sp(2n, \mathbb{R}) \cap O(2n, \mathbb{R})$ is a real symplectic orthogonal matrix, and $\mathbf{R} \in Sp(2n, \mathbb{R}) \cap \text{Sym}^+(2n)$ is a real symplectic symmetric positive definite matrix. Physically, the matrix \mathbf{U} represents passive optical transformations, namely beam-splitters and phase shifters. The matrix \mathbf{R} then includes any single and two-mode squeezing interactions. An equivalent form $\mathbf{U}\mathbf{R}$ of the scattering matrix is provided by the right polar decomposition, where \mathbf{R} and \mathbf{U} are in general distinct from the left polar decomposition.

Generally the polar decomposition leads to dense and complicated matrices \mathbf{R} and \mathbf{U} . Remarkably, we find that the scattering matrix describing our three mode system has extremely simple forms for the left and/or right polar decomposition at points of perfect nonreciprocal scattering, $\mathcal{N}^{(1,2)} = 1$, up to a global change in phase on the scattering matrix, $-\mathbf{S}$. Due to the structure of the covariance matrix, see Eq. (10), this change of phase will not effect the resulting covariances. In these simple cases the \mathbf{R} and \mathbf{U} matrices involve only a single interaction between one pair of modes. The polar decomposition when $\mathcal{N}^{(1,2)} = 1$ is then comprised of symplectic matrices corresponding to the following two unitary operations:

$$\begin{aligned} \mathbf{U}^{(1,3)} &\leftrightarrow \exp \left[2i \arctan \left(\sqrt{\mathcal{C}_{13}} \right) \left(\hat{a}_1^\dagger \hat{a}_3 + \hat{a}_1 \hat{a}_3^\dagger \right) \right] \\ \mathbf{R}^{(2,3)} &\leftrightarrow \exp \left[-2 \operatorname{artanh} \left(\sqrt{\mathcal{C}_{23}} \right) \left(\hat{a}_2^\dagger \hat{a}_3^\dagger - \hat{a}_2 \hat{a}_3 \right) \right]. \end{aligned} \quad (7)$$

Crucially, we find that both left and right polar decompositions can provide useful, complementary insight into the action of the three-mode system at points of perfect nonreciprocal scattering. For the loop phase $\phi = -\pi/2$ it is the left polar decomposition which takes on a simple form:

$$-\mathbf{S} = \mathbf{R}^{(2,3)} \mathbf{U}^{(1,3)} \text{ when } \phi = -\frac{\pi}{2}. \quad (8)$$

As illustrated in Fig. 2, modes a_1 and a_3 interact first via a beam-splitter $\mathbf{U}^{(1,3)}$ which acts to exchange input from a_1 to a_3 , and vice versa. This operation is followed by a two-mode squeezer $\mathbf{R}^{(2,3)}$ between modes a_2 and a_3 ,

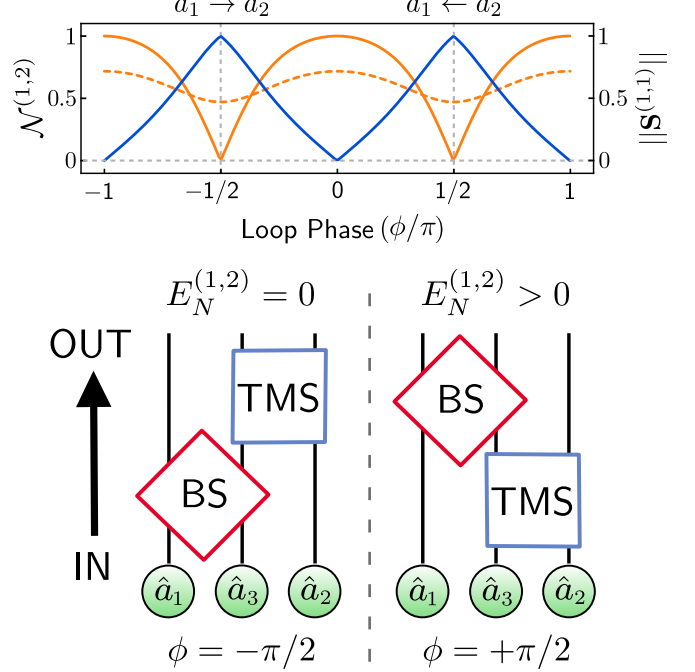


FIG. 2. Top: Scattering properties of the nonreciprocal loop as a function of loop phase ϕ . $\mathcal{N}^{(1,2)}$ is plotted in blue for the impedance matched case only; the general case is qualitatively similar and is omitted for clarity. $\|\mathbf{S}^{(1,1)}\|$ is plotted in orange for the impedance matched (solid) and general (dashed) cases. Lower panels show circuit descriptions of the nonreciprocal system at points of perfect nonreciprocal scattering, where $\mathcal{N}^{(1,2)} = 1$. This description holds regardless of the value of $\|\mathbf{S}^{(1,1)}\|$. The left diagram corresponds to $\phi = -\pi/2$ which yields perfect nonreciprocal scattering in the $a_1 \rightarrow a_2$ direction, while the right diagram corresponds to $\phi = \pi/2$ where scattering is only allowed in the $a_1 \leftarrow a_2$ direction. Input is initially uncorrelated and moves from bottom to top.

where the output of mode a_2 then becomes dependent on the input of mode a_1 , thus realizing directional transmission from $a_1 \rightarrow a_2$. The output of mode a_1 cannot have any dependence on input of a_2 because it can only arrive at the output of mode a_3 via the same two-mode squeezer.

For the opposite sign of the loop phase, $\phi = +\pi/2$, the right polar decomposition yields

$$-\mathbf{S} = \mathbf{U}^{(1,3)} \mathbf{R}^{(2,3)} \text{ when } \phi = \frac{\pi}{2}, \quad (9)$$

which describes the same component operations as Eq. (8) but applied in *reverse* order. As a result, the scattering behaviour is reversed and still nonreciprocal, allowing transmission from $a_1 \leftarrow a_2$.

The relatively simple form of these circuits provide a heuristic picture of nonreciprocal scattering in this system, where changing the direction of the nonreciprocal scattering is equivalent to changing the order of operations in the circuit. However, note that the nonreciprocal behaviour is not explained just by sequential beam-splitters, but also involves two-mode squeezing interac-

tions. This already hints at the possibility of generating nontrivial quantum correlations in scattered output fields, and thus connects to entangling properties of the three-mode system, as we see in the following section.

IV. OUTPUT ENTANGLEMENT AND PURITY

The output state of the three-mode system, and all of its entangling capabilities, is completely characterized by the generally frequency-dependent covariance matrix of the output field quadrature operators, $\mathbf{V}[\omega]$, which can be calculated using Eq. (4) and the knowledge of the input field correlations. The output covariance matrix can then be written in terms of the scattering matrix

$$\mathbf{V}[\omega] = \frac{1}{2} (\mathbf{S}[\omega] \mathbf{V}_{\text{in}} \mathbf{S}^T[-\omega] + \mathbf{S}[-\omega] \mathbf{V}_{\text{in}} \mathbf{S}^T[\omega]), \quad (10)$$

where \mathbf{V}_{in} is the matrix of correlations of the input fields. Assuming the input noise for different modes is uncorrelated, \mathbf{V}_{in} contains variances determined by the thermal occupation number n_k^{th} and vacuum fluctuations (see Appendix A),

$$\mathbf{V}_{\text{in}} = \bigoplus_{k=1}^n \left(n_k^{\text{th}} + \frac{1}{2} \right) \begin{bmatrix} 1 & 0 \\ 0 & 1 \end{bmatrix}. \quad (11)$$

Once again assuming steady-state operation, we set $\omega = 0$ in Eq. (10) so that the covariance matrix of interest, $\mathbf{V}[0] \equiv \mathbf{V}$, takes the simple form:

$$\mathbf{V} = \mathbf{S} \mathbf{V}_{\text{in}} \mathbf{S}^T. \quad (12)$$

From this covariance matrix, we aim to calculate useful entanglement metrics for different bipartitions of the output fields in order to investigate the effects of the nonreciprocal scattering. These include the Simon-Peres-Horodecki criterion for separability of Gaussian states [47], as well as the logarithmic negativity entanglement monotone, denoted by $E_N^{(j,k)}$ [43, 48] for the outputs of the mode pair (j, k) . The latter may be calculated from the minimum symplectic eigenvalue $\nu_-^{(j,k)}$ of the corresponding partially transposed two-mode block $\mathbf{V}^{(j,k)}$ of the total covariance matrix \mathbf{V} via

$$E_N^{(j,k)} = \begin{cases} 0 & \text{for } 2\nu_-^{(j,k)} \geq 1 \\ -\log(2\nu_-^{(j,k)}) & \text{for } 2\nu_-^{(j,k)} < 1 \end{cases}. \quad (13)$$

Similarly, we can define the marginal purity $\mu^{(j,k)}$ of a given bipartition of the output field of modes using

$$\mu^{(j,k)} = \frac{1}{4\sqrt{\det \mathbf{V}^{(j,k)}}}. \quad (14)$$

This measure has a maximum value of $\mu^{(j,k)} = 1$ only for pure states; for mixed states the purity will be $\mu^{(j,k)} < 1$.

A. Entanglement and Purity in a Nonreciprocal System

We begin by examining the entanglement properties and purity of output fields under vacuum input, $n_k^{\text{th}} = 0$, for all modes. In this instance the initial matrix of correlations is comprised of vacuum noise and is therefore the identity matrix, $\mathbf{V}_{\text{in}} = \mathbf{I}_6/2$, so the output covariance matrix is $\mathbf{V} = \frac{1}{2} \mathbf{S} \mathbf{S}^T$. Balancing the cooperativities $\mathcal{C}_{12} = \mathcal{C}_{13} \mathcal{C}_{23}$, we plot the logarithmic negativity between the output of modes a_1 and a_2 , $E_N^{(1,2)}$, as well as $E_N^{(2,3)}$, in the top panel of Fig. 3 where we notice the strong dependence on the value of the loop phase. The simple form for the circuit decomposition means that the behaviour of the entanglement at the points of perfect nonreciprocal scattering between modes a_1 and a_2 , corresponding to the points where $\phi = \pm\pi/2$ in Fig. 3, can be explained simply as follows.

The covariance matrix for the $a_1 \rightarrow a_2$ direction of perfect nonreciprocal scattering may be written using the form of the scattering matrix from Eq. (8)

$$\mathbf{V} = \frac{1}{2} \mathbf{R}^{(2,3)} (\mathbf{R}^{(2,3)})^T \quad (15)$$

where the beam-splitter component does not appear because it is an orthogonal transformation. The entangling behaviour for this direction of the nonreciprocal scattering is therefore equivalent to a two-mode squeezer between modes a_2 and a_3 , and so we must have $E^{(2,3)} > 0$. Since mode a_1 and a_2 share no squeezing, there will be no entanglement generated between these two modes, which is evident in Fig. 3.

We can then ask whether there are other operating points where the entanglement between the output of modes a_1 and a_2 vanishes. This can be determined from the Simon-Peres-Horodecki criterion for the separability of the outputs of modes a_1 and a_2 ; from this criterion it follows that the output fields are separable so long as the following inequality is satisfied:

$$\sqrt{\frac{\mathcal{C}_{12}}{\mathcal{C}_{13} \mathcal{C}_{23}}} + \sqrt{\frac{\mathcal{C}_{13} \mathcal{C}_{23}}{\mathcal{C}_{12}}} \leq -2 \sin \phi, \quad (16)$$

which holds for *all* possible system parameters, and not just at the points of perfect nonreciprocity. This inequality is only satisfied for one set of parameters, $\mathcal{C}_{12} = \mathcal{C}_{13} \mathcal{C}_{23}$ and $\phi = -\pi/2$, which is the point of perfect nonreciprocal scattering where $a_1 \rightarrow a_2$. This is then the only point of operation where the entanglement of the output of modes a_1 and a_2 vanishes, $E^{(1,2)} = 0$. Away from this point the output for these two modes will always be entangled.

For the reverse direction, $a_1 \leftarrow a_2$ we can use Eq. (9) to write the covariance matrix as

$$\mathbf{V} = \frac{1}{2} \mathbf{U}^{(1,3)} \mathbf{R}^{(2,3)} (\mathbf{R}^{(2,3)})^T (\mathbf{U}^{(1,3)})^T. \quad (17)$$

Importantly, the beam-splitter between modes a_1 and a_3 appears and therefore plays an important role in the entanglement generation here. The two-mode squeezer acts

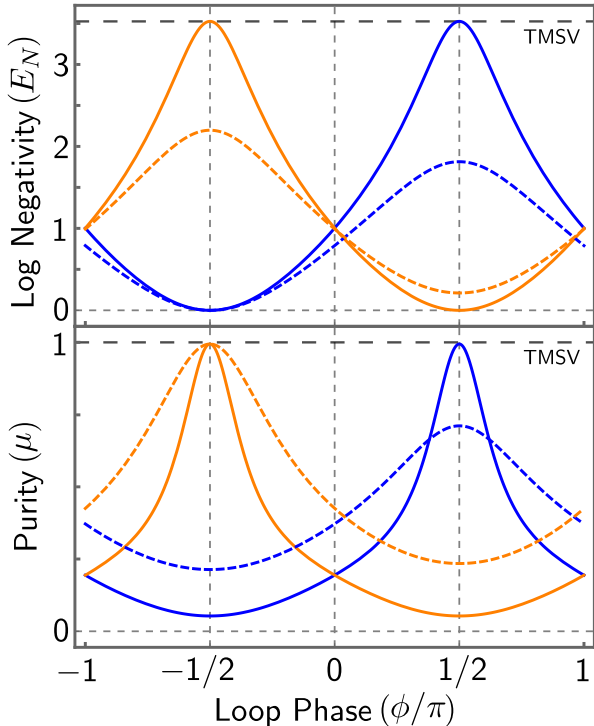


FIG. 3. Logarithmic negativity $E_N^{(i,j)}$ (top) and purity $\mu^{(i,j)}$ (bottom) of the stationary output states when $\mathcal{C}_{12} = \mathcal{C}_{13}\mathcal{C}_{23}$ as a function of the loop phase. The results for the joint states of the outputs of modes a_1 and a_2 (blue) and a_2 and a_3 (orange) are displayed, for two parameter choices: ‘symmetric,’ $\mathcal{C}_{23} = \mathcal{C}_{12}, \mathcal{C}_{13} = 1$ (solid) and ‘asymmetric,’ $\mathcal{C}_{23} = \mathcal{C}_{12}/2, \mathcal{C}_{13} = 2$ (dashed), with $\mathcal{C}_{12} = 0.5$ in both cases. All baths are in the vacuum state. The dashed black lines at top of plots give results for the output state of a *reciprocal* two-mode squeezed system with vacuum input (TMSV), $\mathcal{C}_{23} = \mathcal{C}_{13} = 0$.

first to entangle modes a_2 and a_3 , while the later action of the beam-splitter swaps some of these squeezed correlations from mode a_3 to a_1 , generating entanglement between the output of modes a_1 and a_2 . This resembles the dissipative entanglement protocol [11, 37], where the entanglement of two modes is mediated by a strongly damped auxiliary mode.

Moreover, at $\phi = \pi/2$ there exists only one specific mode of operation where the additional entanglement between mode a_2 and a_3 vanishes: when $\mathcal{C}_{13} = 1$ the beam-splitter in Eq. (7) acts to *perfectly* swap all squeezing from mode a_3 to a_1 , and swap all the uncorrelated vacuum noise from mode a_1 to a_3 . The result of this perfect swap is that a_1 and a_2 now form a two-mode squeezed vacuum state, so the value of $E_N^{(1,2)}$ will be equivalent to the value achieved by a TMS, as seen in Fig. 3. Since modes a_2 and a_3 no longer share any squeezed correlations their measure of entanglement must vanish, $E_N^{(2,3)} = 0$.

In order to discuss the behaviour of $E_N^{(2,3)}$ in more detail we again use the Simon-Peres-Horodecki criterion: the output of a_2 and a_3 will be separable so long as the

following inequality is satisfied:

$$\sqrt{\frac{\mathcal{C}_{23}}{\mathcal{C}_{12}\mathcal{C}_{13}}} + \sqrt{\frac{\mathcal{C}_{12}\mathcal{C}_{13}}{\mathcal{C}_{23}}} \leq 2 \sin \phi. \quad (18)$$

Referring to Eq. (6), it is evident that this is only satisfied when there is nonreciprocal scattering with direction $a_2 \leftarrow a_3$. The required phase here is $\phi = +\pi/2$ which is the *opposite* phase requirement from Eq. (16).

It is evident that the direction of the nonreciprocal scattering, and therefore the value of the phase ϕ , plays a crucial role in the behaviour of the output field entanglement, as depicted in Fig. 3. $E_N^{(1,2)}$ and $E_N^{(2,3)}$ reach maximum values for this parameter regime, where they can both realize the same entangling power of a reciprocal two-mode squeezer, however the maxima are achieved at different values of the phase. In addition this is also the only operating regime where both $E_N^{(1,2)}$ and $E_N^{(2,3)}$ reach the absolute minimum value of 0.

Since both $E_N^{(1,2)}$ and $E_N^{(2,3)}$ vanish when $\mathcal{C}_{12} = \mathcal{C}_{23}$ and $\mathcal{C}_{13} = 1$ it follows that $\mathcal{N}^{(1,2)} = 1$ and $\mathcal{N}^{(2,3)} = 1$, and so both scattering processes are perfectly nonreciprocal. Note that at the point of perfect swapping observed in Eq. (17) the scattering of modes a_1 and a_3 are both impedance matched (see Appendix B) so the input noise is not reflected in the output fields. We will refer to the regime where $\mathcal{C}_{13} = 1$ as the ‘symmetric’ case since $\mathcal{C}_{12} = \mathcal{C}_{23}$. We therefore label the regime where $\mathcal{C}_{13} \neq 1$ the ‘asymmetric’ case. The degree of impedance on mode a_1 is presented in the top plot in Fig. 2, where we see that the reflection of mode a_1 vanishes, i.e. $\|\mathbf{S}^{(1,1)}\| = 0$, only in the symmetric case.

The circuit decomposition also allows for a heuristic explanation of the behaviour of the marginal purities, seen in the bottom plot in Fig. 3. Since the initial covariance matrix is $\mathbf{V}_{\text{in}} = \mathbf{I}_6/2$ for vacuum inputs, the marginal purities for the input states will be $\mu^{(1,2)} = 1$ and $\mu^{(2,3)} = 1$. These purities will remain unchanged in the output state provided the 2-mode block can be reached by a symplectic transformation. This follows since the determinant of a symplectic transformation is $\det(\mathbf{S}) = 1$, and therefore $\det(\mathbf{S}\mathbf{V}\mathbf{S}^T) = \det(\mathbf{V})$.

Since the covariance matrix for $\phi = -\pi/2$, Eq. (15), simply describes a two-mode squeezing interaction between modes a_2 and a_3 , the marginal purity will always remain the same for the, $\mu^{(2,3)} = 1$. On the other hand, the marginal purity of the output state between modes a_1 and a_2 is below one $\mu^{(1,2)} < 1$ in this case, as the 2-mode block $\mathbf{V}^{(1,2)}$ cannot be reached by any combination of symplectic transformations. This same reasoning applies to the opposite phase $\phi = +\pi/2$, where $\mu^{(2,3)} < 1$ always holds and $\mu^{(1,2)} < 1$ only in the asymmetric case. The exception is the symmetric case, where $\mu^{(1,2)} = 1$ because $\mathbf{V}^{(1,2)}$ is equivalent to the covariance matrix for a two-mode squeezed vacuum state. In fact, the condition that saturates the marginal purity $\mu^{(1,2)} = 1$ is equivalent to Eq. (18).

We have therefore observed and explained how entanglement arises in a nonreciprocal system. Crucially, we

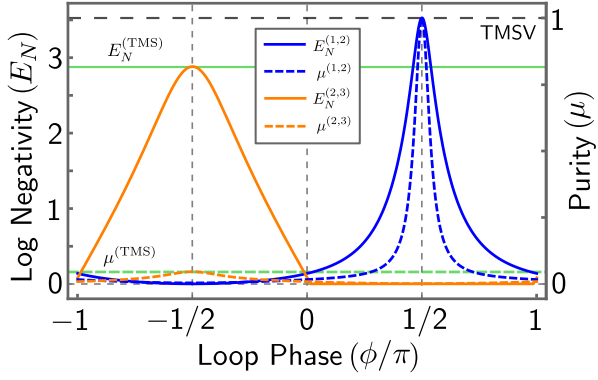


FIG. 4. Logarithmic negativity (solid) and purity (dashed) of output states as a function of the loop phase in the presence of thermal noise. Here $n_1^{\text{th}} = 10$, $n_2^{\text{th}} = n_3^{\text{th}} = 0$, and $\mathcal{C} = 0.5$. The results for the joint output states of modes a_1 and a_2 (blue) and a_2 and a_3 (orange) are displayed. We also display the results for a two-mode squeezed state where $n_1^{\text{th}} = 10$ and $n_2^{\text{th}} = 0$ (green). The dashed black line indicates both the logarithmic negativity and purity for a two-mode squeezed vacuum state (TMSV).

find that the points of perfect nonreciprocity play a special role in maximising achievable output entanglement. We also note how the special symmetric case allows for the purity of the output states to be maximised. We are now in a position to analyze the role of nonreciprocity in entanglement generation in the presence of thermal fluctuations.

V. OUTPUT ENTANGLEMENT IN THE PRESENCE OF THERMAL NOISE

Thermal noise is an unwanted feature when attempting to generate entanglement. In the case of a reciprocal two-mode squeezer, thermal noise incident on one or both modes will only serve to degrade the logarithmic negativity. While this can be overcome by increasing the strength of the two-mode squeezing interaction (e.g. in parametric cQED, using stronger pump strengths), the same is not true for the purity of the generated output state. More precisely, the purity for a two-mode squeezed system where the thermal noise at the inputs for both modes is n_1^{th} and n_2^{th} is given by $\mu^{(1,2)} = 1/(2n_1^{\text{th}} + 1)(2n_2^{\text{th}} + 1)$ which is independent of the degree of squeezing.

One might expect that reciprocally coupling an auxiliary cold mode to the hot modes of interest would help in mitigating this impact. However, while such a coupling can reduce the internal occupation of the hot modes, it is unable to continuously route thermal inputs in a specified direction: away from the propagating output fields. Combining this cold auxiliary mode with nonreciprocity, on the other hand, enables unidirectional scattering of coherent input signals which extends to the routing of thermal fluctuations.

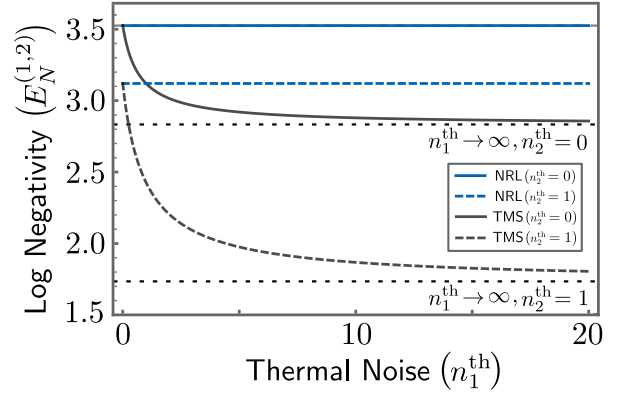


FIG. 5. Entanglement between the stationary output of the modes a_1 and a_2 as measured by the logarithmic negativity, as a function of thermal input noise strength on mode a_1 . We compare the results from an open two-mode squeezed system (TMS, grey) with our nonreciprocal three mode loop (NRL, blue). In both cases the squeezing interaction between modes a_1 and a_2 has cooperativity $\mathcal{C}_{12} = 0.5$. The nonreciprocal loop also has $\mathcal{C}_{23} = 0.5$, $\mathcal{C}_{13} = 1$, and $\phi = +\pi/2$. The thermal occupation of mode a_2 is taken to be $n_2 = 0$ (solid) and $n_2 = 1$ (dashed). Mode a_3 is always taken to have vacuum input. The dashed black lines correspond to the logarithmic negativity for a TMS where $n_1 \rightarrow \infty$ and $n_2 = 0, 1$.

A. Rerouting thermal fluctuations using nonreciprocity

The nonreciprocal loop provides a way for us to avoid these effects on the state shared between the output of modes a_1 and a_2 by setting the parameters to the symmetric case where the scattering of modes a_1 and a_3 are both impedance matched. Provided that the input of mode a_3 is vacuum noise, if we set $\phi = +\pi/2$, thermal noise in the input of mode a_1 can be rerouted to the output of mode a_3 . Due to the presence of thermal noise, the initial covariance matrix is no longer proportional to the identity matrix, and so the output covariance matrix has the following form:

$$\mathbf{V} = \mathbf{U}_{\text{swap}}^{(1,3)} \mathbf{R}^{(2,3)} \mathbf{V}_{\text{in}} (\mathbf{R}^{(2,3)})^T (\mathbf{U}_{\text{swap}}^{(1,3)})^T. \quad (19)$$

However, the circuit description shown in Fig. 2 still holds: modes a_2 and a_3 are entangled and the subsequent beam-splitter acts as a perfect swap between modes a_1 and a_3 . Since $n_1^{\text{th}} \neq 0$, the output of mode a_3 will receive the unwanted thermal noise while the output of mode a_1 forms a two-mode squeezed state with mode a_2 . Provided the input for mode a_2 is also vacuum noise, then the $(1, 2)$ state will be a two-mode squeezed vacuum state with maximum purity and entanglement, unaffected by the value of n_1^{th} , as seen in Fig. 4 (see Appendix C for details of scattering behaviour).

At this point of operation, a complementary circuit description can be obtained using the *right* polar decomposition of the scattering matrix instead, which also takes

on a simple form,

$$-\mathbf{S} = \mathbf{R}^{(1,2)} \mathbf{U}_{\text{swap}}^{(1,3)} \text{ when } \phi = +\frac{\pi}{2} \quad (20)$$

where $\mathbf{U}_{\text{swap}}^{(1,3)}$ is the beam-splitter operation from Eq. (7) where $\mathcal{C}_{13} = 1$, and $\mathbf{R}^{(1,2)}$ is a two-mode squeezing operation between modes a_1 and a_2

$$\mathbf{R}^{(1,2)} \leftrightarrow \exp \left[2i \operatorname{artanh} \left(\sqrt{\mathcal{C}_{23}} \right) \left(\hat{a}_1^\dagger \hat{a}_2^\dagger + \hat{a}_1 \hat{a}_2 \right) \right]. \quad (21)$$

Then, we can write the covariance matrix described by Eq. (19) in an equivalent form

$$\mathbf{V} = \mathbf{R}^{(1,2)} \mathbf{U}_{\text{swap}}^{(1,3)} \mathbf{V}_{\text{in}} (\mathbf{U}_{\text{swap}}^{(1,3)})^T (\mathbf{R}^{(1,2)})^T. \quad (22)$$

Here the action of the beam-splitter can be seen explicitly on \mathbf{V}_{in} : it swaps the thermal noise from mode a_1 with the vacuum noise input from mode a_3 . This is followed by a two-mode squeezer acting directly to entangle the mode pair $(1, 2)$, creating a state with maximum purity and entanglement. It is important to note that mode a_1 is not cooled using this scheme, and that the nonreciprocal loop only allows for the thermal noise to be rerouted so as to not appear in the output field.

If we tune ϕ away from operating points of perfect nonreciprocity and impedance matching, the entanglement and purity of the mode pair $(1, 2)$ degrade as before. However, comparing Fig. 4 and the previous results when only considering vacuum inputs, Fig. 3, we note that the degradation is more pronounced when the input to mode a_1 is thermal. This observation further highlights the importance of nonreciprocity in implementing perfect swaps of thermal inputs.

Finally, while thermal noise in one mode is detrimental to both entanglement and purity, the effects are compounded when both modes contain some thermal noise input. Fig. 5 demonstrates the effects of incident thermal noise on both modes of an entangled pair. The nonreciprocal loop has the benefit that regardless of the amount of thermal noise incident on mode a_2 , the thermal noise incident on mode a_1 is always swapped away in the output. The usual two-mode squeezed state, on the other hand, will experience extra degradation of the entanglement and purity as n_1^{th} increases for even relatively small values of n_2^{th} .

B. Entangling the Output Fields of Two Hot Modes

The nonreciprocal loop allows for the output fields of one hot and one cold to be entangled with maximum purity. As seen in Fig. 5, when using this system to realise such an entangled state between the output fields of two hot modes, the logarithmic negativity is reduced, since it is only possible to reroute the thermal noise from one of the input modes.

However, it is possible to entangle the outputs of two hot modes if we use two nonreciprocal loops and employ

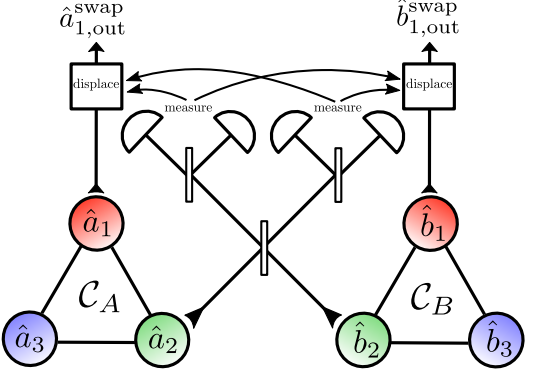


FIG. 6. Schematic for a potential entanglement swapping scheme to entangle the output fields of two hot modes. The scheme begins with two nonreciprocal loops, each comprising a hot primary mode (red), a secondary mode (green) we wish to optimally entangle with the hot mode, and a cold auxiliary mode (blue). As with the setup covered in this paper, the hot and cold auxiliary modes are coupled via a beam-splitter interaction. The other interactions must then be two-mode squeezers. To entangle both hot mode outputs, the output state of the secondary modes is passed through a 50/50 beam-splitter and then measured. The displacement of the output for the hot modes is then conditioned on the measurements; their outputs will then be entangled.

the entanglement swapping protocol [49, 50]. A possible setup is shown in Fig. 6, with two realizations of the NRL (A and B respectively). Two hot modes a_1, b_1 are coupled to cold auxiliary modes a_3, b_3 respectively, with secondary modes a_2, b_2 completing the corresponding loops. Both loops are operated under symmetric configurations and are thus parameterized by a single two-mode squeezing cooperativity each (\mathcal{C}_A and \mathcal{C}_B respectively). In light of our previous results, we also operate at points of perfect nonreciprocal scattering and impedance matching. The loop phase is assumed to be tuned such that the thermal noise incident on the hot mode is routed to the output of the cold auxiliary mode. Provided the input for secondary mode is also in the vacuum state, the output for the hot and secondary modes from each loop will be optimally entangled as a two-mode squeezed vacuum state with maximum purity.

In the swapping protocol, the outputs from the secondary modes are mixed via a beam-splitter and then measured. The outputs for the hot modes are then displaced, conditioned on the result of these measurements. Perfect application of this entanglement swapping protocol would allow for the output fields for the two hot modes to be combined to produce another two-mode squeezed vacuum state with purity $\mu = 1$. The entanglement for the resulting state is then [50]

$$E_N = 2r \text{ where } \tanh(r) = \frac{4\sqrt{\mathcal{C}_A \mathcal{C}_B}}{(1 + \mathcal{C}_A)(1 + \mathcal{C}_B)} \quad (23)$$

which is independent of the thermal noise incident on both hot modes. We therefore see that the entanglement

of the propagating fields from hot modes a_1 and b_1 , and the purity of the generated flying states, can be rendered robust to their thermal inputs using nonreciprocity. ...

VI. CONCLUSIONS AND OUTLOOK

In this paper we have analyzed how engineered nonreciprocity in quantum systems influences their ability to entangle propagating fields incident on their constituent quantum modes. This requires analyzing the role of nonreciprocity beyond asymmetric scattering for signal routing - a notion that can be defined completely classically - and in particular exploring its influence on quantum correlations and steady-state entanglement of fields. Using a minimal system consisting of a two-mode squeezer and where each mode is coupled to a third, auxiliary mode in a closed-loop configuration, we show that the generated entanglement of output fields can depend strongly on the direction of nonreciprocal scattering. It is not *a priori* obvious that it should be possible to entangle outputs from two modes for which signal flow is only unidirectional. However, we have shown that this is indeed possible, given the right configuration of the system.

To explain this somewhat surprising entanglement behaviour, we develop a heuristic picture that is based on a polar decomposition of the scattering matrix. This description maps nonreciprocal scattering to sequential Gaussian circuit operations, including pairwise beam splitters and more importantly two-mode squeezers generating entanglement. This picture then helped us explain a second key result: that engineered nonreciprocity can be used to reroute thermal fluctuations from a hot propagating mode towards the output of the cold auxiliary mode (via the beam-splitter component), while simultaneously allowing the entanglement of propagating output fields (via the two-mode squeezer component). This renders output field entanglement much more robust to thermal fluctuations when compared to a reciprocal two-mode squeezing interaction.

Our work is relevant to the generation of stationary entanglement of itinerant low frequency modes, where thermal occupations can be appreciable even at cryogenic temperatures. Our analysis also brings to light the possible uses of nonreciprocity in entanglement generation. With recent interest in multipartite entanglement in quantum systems of increasing scale, our work invites the exploration of whether engineered nonreciprocity can be a useful resource in improving robustness of multipartite entanglement in low frequency modes.

VII. ACKNOWLEDGEMENTS

The authors thank C. M. Wilson and C. W. Sandbo Chang for useful discussions. AM and LO acknowledge funding by the Deutsche Forschungsgemeinschaft through the project CRC 910 and the Emmy Noether

program (Grant No. ME 4863/1-1). SK acknowledges funding by the Israeli Science Foundation (Grant 1794/21) and the Israeli Innovation Authority (Grant 73754).

Appendix A: Heisenberg-Langevin equations of motion

We work in the quadrature basis, which consists of the position and momentum quadrature operators, $\hat{X}_k = (\hat{a}_k^\dagger + \hat{a}_k)/\sqrt{2}$ and $\hat{P}_k = i(\hat{a}_k^\dagger - \hat{a}_k)/\sqrt{2}$, respectively. The canonical commutation relations have the usual form $[\hat{X}_j, \hat{P}_k] = i\delta_{jk}$. Defining the vector of quadrature operators for the three mode system $\vec{R} = (\hat{X}_1, \hat{P}_1, \hat{X}_2, \hat{P}_2, \hat{X}_3, \hat{P}_3)$, we can write the Heisenberg-Langevin equations as the follows

$$\frac{d}{dt}\vec{R}(t) = \mathbf{M}\vec{R}(t) - \sqrt{\kappa}\vec{R}_{\text{in}}[\omega] \quad (\text{A1})$$

where \mathbf{M} is a time independent dynamical matrix, $\kappa = \text{diag}(\kappa_1, \kappa_1, \kappa_2, \kappa_2, \kappa_3, \kappa_3)$ is a diagonal matrix of the mode damping rates, and \vec{R}_{in} is the vector of input noise operators in the quadrature basis. The correlators of the elements of the matrix \vec{R}_{in} have the form

$$\begin{aligned} \langle \hat{X}_{j,\text{in}}(t)\hat{X}_{k,\text{in}}(t') \rangle &= \delta_{jk} \left(n_j^{\text{th}} + \frac{1}{2} \right) \delta(t - t') \\ \langle \hat{P}_{j,\text{in}}(t)\hat{P}_{k,\text{in}}(t') \rangle &= \delta_{jk} \left(n_j^{\text{th}} + \frac{1}{2} \right) \delta(t - t') \\ \langle \hat{X}_{j,\text{in}}(t)\hat{P}_{k,\text{in}}(t') \rangle &= \delta_{jk} \frac{i}{2} \delta(t - t') \\ \langle \hat{P}_{j,\text{in}}(t)\hat{X}_{k,\text{in}}(t') \rangle &= -\delta_{jk} \frac{i}{2} \delta(t - t'). \end{aligned} \quad (\text{A2})$$

These are white noise processes, and so have a mean of zero. The dynamical matrix for the system can be written as follows:

$$\mathbf{M} = \begin{pmatrix} -\frac{\kappa_1}{2}\mathbf{I} & -g_{12}\mathbf{X} & g_{13}\mathbf{J} \\ -g_{12}\mathbf{X} & -\frac{\kappa_2}{2}\mathbf{I} & g_{23}(\sin\phi\mathbf{Z}) \\ g_{13}\mathbf{J} & g_{23}(\sin\phi\mathbf{Z}) & -\frac{\kappa_3}{2}\mathbf{I} \end{pmatrix} \quad (\text{A3})$$

The linear Heisenberg-Langevin equations of motion, Eq. (A1), can be transformed to frequency space and written in the compact form

$$-i\omega\vec{R}[\omega] = \mathbf{M}\vec{R}[\omega] - \sqrt{\kappa}\vec{R}_{\text{in}}[\omega]. \quad (\text{A4})$$

This linear algebraic system can be straightforwardly solved,

$$\vec{R}[\omega] = -(i\omega + \mathbf{M})^{-1}\sqrt{\kappa}\vec{R}_{\text{in}}[\omega] \quad (\text{A5})$$

Quantum input-output theory [44] relates the output field quadratures to the input and system fields:

$$\vec{R}_{\text{out}}[\omega] = \vec{R}[\omega] - \sqrt{\kappa}\vec{R}_{\text{in}}[\omega] \quad (\text{A6})$$

Using Eq. (A5) then allows us to express the output fields entirely in terms of the input fields, which defines the scattering matrix $\mathbf{S}[\omega]$, as introduced in Eq. (4) of the main text. The covariance matrix for the output modes in frequency space may be written as

$$\mathbf{V}[\omega] = \frac{1}{2} \int_{-\infty}^{\infty} \left\langle \vec{R}_{\text{out}}[\omega] \vec{R}_{\text{out}}[\omega']^T + \vec{R}_{\text{out}}[\omega'] \vec{R}_{\text{out}}[\omega]^T \right\rangle d\omega' \quad (\text{A7})$$

where we take the outer product of the \vec{R}_{out} vectors. The above can be rewritten in terms of the input fields and scattering matrix using Eq. (4), and the correlators of the input fields may be calculated using the frequency space version of the correlators from Eq. (A2), where the

Fourier transform replaces $\delta(t - t')$ with $\delta(\omega + \omega')$.

Appendix B: Block form of full scattering matrix

Using Eq. (A5) in conjunction with Eq. (A6) allows us to obtain the full, frequency-dependent scattering matrix of the three mode system. However, as discussed in the main text, we are typically interested in scattering properties at $\omega = 0$. Furthermore, we have also discussed how the simplest intuitive scattering behaviour can be analyzed in the symmetric, impedance-matched case defined by $\mathcal{C}_{12}, \mathcal{C}_{23} \equiv \mathcal{C}$, and $\mathcal{C}_{13} = 1$. In this case, $\mathbf{S}[0] \equiv \mathbf{S}$ is determined entirely by \mathcal{C} and the loop phase ϕ , and takes the form:

$$\mathbf{S} = \begin{pmatrix} \mathbf{S}^{(1,1)} & \mathbf{S}^{(1,2)} & \mathbf{S}^{(1,3)} \\ \mathbf{S}^{(2,1)} & \mathbf{S}^{(2,2)} & \mathbf{S}^{(2,3)} \\ \mathbf{S}^{(3,1)} & \mathbf{S}^{(3,2)} & \mathbf{S}^{(3,3)} \end{pmatrix} \equiv D(\phi) \begin{pmatrix} \mathbf{F}(\phi) \cos \phi & \mathbf{B}(\phi)(1 + \sin \phi) & \mathbf{A}(\phi) \\ \mathbf{B}(\phi - \pi)(1 - \sin \phi) & -(1 - \mathcal{C}^2)\mathbf{I} + \bar{\mathbf{F}}(\phi) \cos \phi & \mathbf{C}(\phi)(1 + \sin \phi) \\ \mathbf{A}(-\phi) & \bar{\mathbf{C}}(-\phi)(1 - \sin \phi) & \mathbf{F}(\phi) \cos \phi \end{pmatrix} \quad (\text{B1})$$

Here $D(\phi) = (1 - \mathcal{C})^2 + \mathcal{C}^2 \cos^2 \phi$ is an overall multiplicative factor that does not influence the nonreciprocity of scattering. The diagonal terms describing reflections take the form:

$$\begin{aligned} \mathbf{F}(\phi) &= \mathcal{C}^2 \cos(\phi) \mathbf{I} - (1 - \mathcal{C})\mathcal{C} \mathbf{J} \\ \bar{\mathbf{F}}(\phi) &= \mathcal{C}^2 \cos(\phi) \mathbf{I} + 2\mathcal{C} \mathbf{J} \end{aligned} \quad (\text{B2})$$

The off-diagonal terms that describe transmission between modes take the form:

$$\begin{aligned} \mathbf{B}(\phi) &= \sqrt{\mathcal{C}} \frac{\cos \phi(1 + \mathcal{C} \sin \phi)}{1 + \sin \phi} \mathbf{Z} \\ &\quad - \sqrt{\mathcal{C}}(2\mathcal{C} - \mathcal{C} \sin \phi - 1) \mathbf{X} \end{aligned} \quad (\text{B3})$$

The interaction between modes a_1 and a_3 is a beam-splitter and is compactly described by a single ϕ -dependent matrix $\mathbf{A}(\phi)$:

$$\begin{aligned} \mathbf{A}(\phi) &= \mathcal{C}^2 \cos \phi(1 + \sin \phi) \mathbf{I} \\ &\quad - \mathcal{C}^2 \cos^2 \phi - (1 - \mathcal{C})(1 + \mathcal{C} \sin \phi) \mathbf{J} \end{aligned} \quad (\text{B4})$$

From Eq. (B1), it is now straightforward to read off conditions for specific desired scattering properties. For example, impedance matching of mode a_1 demands $\|\mathbf{S}^{(1,1)}\| = 0$, which clearly requires $\cos \phi = 0 \implies \phi = \pm\pi/2$. Similarly, perfect nonreciprocal scattering between modes a_1 and a_2 as defined in Eq. (5) of the main text, $\mathcal{N}^{(1,2)} = 1$, clearly requires $(1 \pm \sin \phi) = 0$, which again implies $\phi = \pm\pi/2$. These are the conditions shown in Fig. 2.

Appendix C: Scattering Properties

When the NRL is optimised to allow swapping of thermal noise from mode a_1 to mode a_3 , we use the impedance-matched case from the previous section, additionally setting the phase to $\phi = \pi/2$. In the quadrature basis the steady-state scattering matrix will have the following form:

$$\mathbf{S}_{\text{NRL}} = \begin{pmatrix} \mathbf{0} & \frac{\sqrt{\mathcal{C}}}{1 - \mathcal{C}} \mathbf{X} & -\frac{1 + \mathcal{C}}{1 - \mathcal{C}} \mathbf{J} \\ \mathbf{0} & -\frac{1 + \mathcal{C}}{1 - \mathcal{C}} \mathbf{I} & -\frac{\sqrt{\mathcal{C}}}{1 - \mathcal{C}} \mathbf{Z} \\ -\mathbf{J} & \mathbf{0} & \mathbf{0} \end{pmatrix} \quad (\text{C1})$$

where we have written the matrix in block form using the following 2×2 matrices

$$\mathbf{X} = \begin{pmatrix} 0 & 1 \\ 1 & 0 \end{pmatrix} \quad \mathbf{Z} = \begin{pmatrix} 1 & 0 \\ 0 & -1 \end{pmatrix} \quad \mathbf{J} = \begin{pmatrix} 0 & 1 \\ -1 & 0 \end{pmatrix} \quad (\text{C2})$$

where \mathbf{I} is the identity and $\mathbf{0}$ is the zero matrix. Replacing the cooperativity with the following squeezing parameter $r = \text{artanh}[2\sqrt{\mathcal{C}}/(1 + \mathcal{C})]$ we can rewrite the scattering matrix as follows

$$\mathbf{S}_{\text{NRL}} \equiv \begin{pmatrix} \mathbf{0} & \sinh(r) \mathbf{X} & -\cosh(r) \mathbf{J} \\ \mathbf{0} & -\cosh(r) \mathbf{I} & -\sinh(r) \mathbf{Z} \\ -\mathbf{J} & \mathbf{0} & \mathbf{0} \end{pmatrix} \quad (\text{C3})$$

This makes clear the behaviour of the system at this point of nonreciprocity. Modes a_1 and a_2 are independent of

the input noise on mode a_1 , which only appears in mode a_3 showing how the noise is rerouted there. Meanwhile, modes a_2 and a_3 share some squeezed correlations.

We can also calculate the steady-state scattering matrix for an open system with a TMS Hamiltonian given by $ig(\hat{a}_1^\dagger \hat{a}_2^\dagger - \hat{a}_1 \hat{a}_2)$ (choosing the TMS phase to be zero as in Eqn. 1 is not appropriate here; this comes from the polar decomposition):

$$\mathbf{S}_{\text{TMS}} = \begin{pmatrix} -\frac{1+\mathcal{C}}{1-\mathcal{C}} \mathbf{I} & -\frac{2\sqrt{\mathcal{C}}}{1-\mathcal{C}} \mathbf{Z} \\ -\frac{2\sqrt{\mathcal{C}}}{1-\mathcal{C}} \mathbf{Z} & -\frac{1+\mathcal{C}}{1-\mathcal{C}} \mathbf{I} \end{pmatrix} \quad (\text{C4})$$

Defining the squeezing in the same way we arrive at the following scattering matrix

$$\mathbf{S}_{\text{TMS}} \equiv \begin{pmatrix} -\cosh(r) \mathbf{I} & -\sinh(r) \mathbf{Z} \\ -\sinh(r) \mathbf{Z} & -\cosh(r) \mathbf{I} \end{pmatrix} \quad (\text{C5})$$

While the covariance matrix of the TMS and modes a_1 and a_2 in the NRL will be identical, the scattering behaviour is markedly different. This is expected given the circuit decomposition for the NRL; since the squeezing is swapped from mode a_3 to mode a_1 by a beam-splitter, the quadratures are rotated during this swap in a manner that cannot be replicated in a TMS alone.

Appendix D: Stability Conditions

We provide below the Routh-Hurwitz stability criterion for the three mode loop at the phases $\phi = \pm\pi/2$:

$$\begin{aligned} 0 &< \kappa_1 + \kappa_2 + \kappa_3 \\ 0 &< 1 - \mathcal{C}_{12} + \mathcal{C}_{13} - \mathcal{C}_{23} \\ 0 &< 1 - \frac{\mathcal{C}_{12}}{(1 + \kappa_3/\kappa_1)(1 + \kappa_3/\kappa_2)} + \frac{\mathcal{C}_{13}}{(1 + \kappa_2/\kappa_1)(1 + \kappa_2/\kappa_3)} \\ &\quad - \frac{\mathcal{C}_{23}}{(1 + \kappa_1/\kappa_2)(1 + \kappa_1/\kappa_3)} \end{aligned} \quad (\text{D1})$$

Away from these phases there are more conditions which must be met, and the conditions in general take on a much more complicated form. Provided the cooperativities and dissipation rates are chosen appropriately the system can be stable across for all values of the loop phase.

In case we also apply the condition $\mathcal{C}_{12} = \mathcal{C}_{13}\mathcal{C}_{23}$ to make the system nonreciprocal, the second listed condition takes on a much simpler form

$$0 < (1 - \mathcal{C}_{23})(1 + \mathcal{C}_{13}) \quad (\text{D2})$$

The system is naturally stable for all choices of the beam-splitter cooperativity, and is therefore limited by the free two-mode squeezing cooperativity $\mathcal{C}_{23} < 1$ which is identical to the stability criterion for an open two-mode squeezer. The two-mode squeezing cooperativity fixed by the nonreciprocity condition, \mathcal{C}_{12} , can therefore grow quite large with the system remaining stable. Provided the dissipation rates are chosen correctly, the other conditions can be satisfied as well.

[1] R. Horodecki, P. Horodecki, M. Horodecki, and K. Horodecki, Quantum entanglement, *Reviews of Modern Physics* **81**, 865 (2009), publisher: American Physical Society.

[2] H. J. Kimble, The quantum internet, *Nature* **453**, 1023 (2008), number: 7198 Publisher: Nature Publishing Group.

[3] J. I. Cirac, P. Zoller, H. J. Kimble, and H. Mabuchi, Quantum State Transfer and Entanglement Distribution among Distant Nodes in a Quantum Network, *Physical Review Letters* **78**, 3221 (1997), publisher: American Physical Society.

[4] A. Acín, J. I. Cirac, and M. Lewenstein, Entanglement percolation in quantum networks, *Nature Physics* **3**, 256 (2007), number: 4 Publisher: Nature Publishing Group.

[5] C. Eichler, C. Lang, J. M. Fink, J. Govenius, S. Filipp, and A. Wallraff, Observation of Entanglement between Itinerant Microwave Photons and a Superconducting Qubit, *Physical Review Letters* **109**, 240501 (2012), publisher: American Physical Society.

[6] M. F. Gely, M. Kounalakis, C. Dickel, J. Dalle, R. Vatré, B. Baker, M. D. Jenkins, and G. A. Steele, Observation and stabilization of photonic Fock states in a hot radio-frequency resonator, *Science* **363**, 1072 (2019), publisher: American Association for the Advancement of Science.

[7] J. Li and S. Gröblacher, Stationary quantum entanglement between a massive mechanical membrane and a low frequency LC circuit, *New Journal of Physics* **22**, 063041 (2020), publisher: IOP Publishing.

[8] G. Steele, M. Gely, I. Rodrigues, D. Bothner, M. Kounalakis, C. Dickel, J. Dalle, R. Vatré, B. Baker, and M. Jenkins, Photonics at radio frequency: Quantum sensing of radio-frequency photons and vibrations, in *Optical and Quantum Sensing and Precision Metrology*, Vol. 11700 (SPIE, 2021) p. 117001B.

[9] D. Vitali, S. Gigan, A. Ferreira, H. Böhm, P. Tombesi, A. Guerreiro, V. Vedral, A. Zeilinger, and M. Aspelmeyer, Optomechanical entanglement between a movable mirror and a cavity field, *Physical Review Letters* **98**, 030405 (2007).

[10] C. Genes, A. Mari, P. Tombesi, and D. Vitali, Robust entanglement of a micromechanical resonator with out-

put optical fields, *Physical Review A* **78**, 032316 (2008), publisher: American Physical Society.

[11] Y.-D. Wang, S. Chesi, and A. A. Clerk, Bipartite and tripartite output entanglement in three-mode optomechanical systems, *Physical Review A* **91**, 013807 (2015), publisher: American Physical Society.

[12] A. Bienfait, K. J. Satzinger, Y. Zhong, H.-S. Chang, M.-H. Chou, C. R. Conner, É. Dumur, J. Grebel, G. A. Peairs, R. G. Povey, *et al.*, Phonon-mediated quantum state transfer and remote qubit entanglement, *Science* **364**, 368 (2019).

[13] S. Barzanjeh, E. S. Redchenko, M. Peruzzo, M. Wulf, D. P. Lewis, G. Arnold, and J. M. Fink, Stationary entangled radiation from micromechanical motion, *Nature* **570**, 480 (2019), number: 7762 Publisher: Nature Publishing Group.

[14] J. Chen, M. Rossi, D. Mason, and A. Schliesser, Entanglement of propagating optical modes via a mechanical interface, *Nature Communications* **11**, 943 (2020).

[15] J.-W. Pan, C. Simon, Č. Brukner, and A. Zeilinger, Entanglement purification for quantum communication, *Nature* **410**, 1067 (2001).

[16] L.-M. Duan, G. Giedke, J. I. Cirac, and P. Zoller, Entanglement purification of gaussian continuous variable quantum states, *Phys. Rev. Lett.* **84**, 4002 (2000).

[17] A. Franzen, B. Hage, J. DiGuglielmo, J. Fiurás ek, and R. Schnabel, Experimental demonstration of continuous variable purification of squeezed states, *Phys. Rev. Lett.* **97**, 150505 (2006).

[18] A. Kamal, J. Clarke, and M. Devoret, Noiseless nonreciprocity in a parametric active device, *Nature Physics* **7**, 311 (2011).

[19] K. Sliwa, M. Hatridge, A. Narla, S. Shankar, L. Frunzio, R. Schoelkopf, and M. Devoret, Reconfigurable josephson circulator/directional amplifier, *Physical Review X* **5**, 041020 (2015).

[20] F. Ruesink, M.-A. Miri, A. Alu, and E. Verhagen, Nonreciprocity and magnetic-free isolation based on optomechanical interactions, *Nature communications* **7**, 1 (2016).

[21] F. Lecocq, L. Ranzani, G. Peterson, K. Cicak, R. Simmonds, J. Teufel, and J. Aumentado, Nonreciprocal microwave signal processing with a field-programmable josephson amplifier, *Physical Review Applied* **7**, 024028 (2017).

[22] G. A. Peterson, F. Lecocq, K. Cicak, R. W. Simmonds, J. Aumentado, and J. D. Teufel, Demonstration of efficient nonreciprocity in a microwave optomechanical circuit, *Physical Review X* **7**, 031001 (2017).

[23] B. J. Chapman, E. I. Rosenthal, J. Kerckhoff, B. A. Moores, L. R. Vale, J. Mates, G. C. Hilton, K. Lalumiere, A. Blais, and K. Lehnert, Widely tunable on-chip microwave circulator for superconducting quantum circuits, *Physical Review X* **7**, 041043 (2017).

[24] M.-A. Miri, F. Ruesink, E. Verhagen, and A. Alù, Optical nonreciprocity based on optomechanical coupling, *Physical Review Applied* **7**, 064014 (2017).

[25] K. Fang, J. Luo, A. Metelmann, M. H. Matheny, F. Marquardt, A. A. Clerk, and O. Painter, Generalized nonreciprocity in an optomechanical circuit via synthetic magnetism and reservoir engineering, *Nature Physics* **13**, 465 (2017).

[26] F. Ando, Y. Miyasaka, T. Li, J. Ishizuka, T. Arakawa, Y. Shiota, T. Moriyama, Y. Yanase, and T. Ono, Observation of superconducting diode effect, *Nature* **584**, 373 (2020).

[27] Z. Shen, Y.-L. Zhang, Y. Chen, C.-L. Zou, Y.-F. Xiao, X.-B. Zou, F.-W. Sun, G.-C. Guo, and C.-H. Dong, Experimental realization of optomechanically induced nonreciprocity, *Nature Photonics* **10**, 657 (2016).

[28] N. R. Bernier, L. D. Toth, A. Koottandavida, M. A. Ioannou, D. Malz, A. Nunnenkamp, A. Feofanov, and T. Kippenberg, Nonreciprocal reconfigurable microwave optomechanical circuit, *Nature communications* **8**, 1 (2017).

[29] S. Barzanjeh, M. Wulf, M. Peruzzo, M. Kalae, P. Deterle, O. Painter, and J. M. Fink, Mechanical on-chip microwave circulator, *Nature communications* **8**, 1 (2017).

[30] L. M. de Lépinay, E. Damskägg, C. F. Ockeloen-Korppi, and M. A. Sillanpää, Realization of directional amplification in a microwave optomechanical device, *Physical Review Applied* **11**, 034027 (2019).

[31] H. Xu, L. Jiang, A. Clerk, and J. Harris, Nonreciprocal control and cooling of phonon modes in an optomechanical system, *Nature* **568**, 65 (2019).

[32] C.-H. Dong, Z. Shen, C.-L. Zou, Y.-L. Zhang, W. Fu, and G.-C. Guo, Brillouin-scattering-induced transparency and non-reciprocal light storage, *Nature communications* **6**, 1 (2015).

[33] J. Kim, M. C. Kuzyk, K. Han, H. Wang, and G. Bahl, Non-reciprocal brillouin scattering induced transparency, *Nature Physics* **11**, 275 (2015).

[34] A. Metelmann and A. A. Clerk, Nonreciprocal photon transmission and amplification via reservoir engineering, *Phys. Rev. X* **5**, 021025 (2015).

[35] L. Ranzani and J. Aumentado, Graph-based analysis of nonreciprocity in coupled-mode systems, *New Journal of Physics* **17**, 023024 (2015).

[36] A. Metelmann and A. Clerk, Nonreciprocal quantum interactions and devices via autonomous feedforward, *Physical Review A* **95**, 013837 (2017).

[37] Y.-D. Wang and A. A. Clerk, Reservoir-Engineered Entanglement in Optomechanical Systems, *Physical Review Letters* **110**, 253601 (2013), publisher: American Physical Society.

[38] N. E. Frattini, U. Vool, S. Shankar, A. Narla, K. M. Sliwa, and M. H. Devoret, 3-wave mixing Josephson dipole element, *Applied Physics Letters* **110**, 222603 (2017), publisher: American Institute of Physics.

[39] V. Sivak, N. Frattini, V. Joshi, A. Lingenfelter, S. Shankar, and M. Devoret, Kerr-Free Three-Wave Mixing in Superconducting Quantum Circuits, *Physical Review Applied* **11**, 054060 (2019), publisher: American Physical Society.

[40] D. Walls and G. J. Milburn, eds., *Quantum Optics* (Springer, Berlin, Heidelberg, 2008).

[41] G. Liu, X. Cao, T.-C. Chien, C. Zhou, P. Lu, and M. Hatridge, Noise reduction in qubit readout with a two-mode squeezed interferometer, *arXiv preprint arXiv:2007.15460* (2020).

[42] J. Y. Qiu, A. Grimsmo, K. Peng, B. Kannan, B. Lienhard, Y. Sung, P. Krantz, V. Bolkhovsky, G. Calusine, D. Kim, *et al.*, Broadband squeezed microwaves and amplification with a josephson traveling-wave parametric amplifier, *arXiv preprint arXiv:2201.11261* (2022).

[43] C. Weedbrook, S. Pirandola, R. García-Patrón, N. J.

Cerf, T. C. Ralph, J. H. Shapiro, and S. Lloyd, Gaussian quantum information, *Reviews of Modern Physics* **84**, 621 (2012).

[44] C. W. Gardiner and M. J. Collett, Input and output in damped quantum systems: Quantum stochastic differential equations and the master equation, *Physical Review A* **31**, 3761 (1985).

[45] S. L. Braunstein, Squeezing as an irreducible resource, *Physical Review A* **71**, 055801 (2005).

[46] M. A. d. Gosson, *Symplectic Methods in Harmonic Analysis and in Mathematical Physics*, 1st ed. (Birkhäuser, Basel, 2011).

[47] R. Simon, Peres-horodecki separability criterion for continuous variable systems, *Physical Review Letters* **84**, 2726 (2000).

[48] G. Vidal and R. F. Werner, Computable measure of entanglement, *Physical Review A* **65**, 032314 (2002).

[49] J. Hoelscher-Obermaier and P. van Loock, Optimal gaussian entanglement swapping, *Physical Review A* **83**, 012319 (2011).

[50] P. van Loock, Quantum communication with continuous variables, *Fortschritte der Physik: Progress of Physics* **50**, 1177 (2002).